A Reformed Empirical Equation for the Discharge Coefficient of Free-Flowing Type-A Piano Key Weirs

Subhojit Kadia[1]; Elena Pummer[2]; Binit Kumar[3]; Nils Rüther[4]; and Zulfequar Ahmad[5]

[1]PhD Candidate, Department of Civil and Environmental Engineering, Norwegian University of Science and Technology, 7491 Trondheim, Norway, Email: subhojit.kadia@ntnu.no, subhojitkadia@gmail.com, ORCID ID 0000-0002-9134-3222 (corresponding author)

[2]Associate Professor, Department of Civil and Environmental Engineering, Norwegian University of Science and Technology, 7491 Trondheim, Norway, Email: elena.pummer@ntnu.no, ORCID ID 0000-0002-0255-4715

[3]Formerly Research Scholar, Department of Civil Engineering, Indian Institute of Technology Roorkee, Uttarakhand 247667, India, Email: binit.nit2010@gmail.com, ORCID ID 0000-0002-3911-7105

[4]Professor, Chair of Hydraulic Engineering, Technical University of Munich, Arcisstr. 21 80333 Munich, Germany, Email: nils.ruether@tum.de ORCID ID 0000-0002-7667-5966

[5]Professor, Department of Civil Engineering, Indian Institute of Technology Roorkee, Uttarakhand 247667, India, Email: zulfifce@iitr.ac.in

Abstract

The existing equations for the discharge coefficient of Piano key weirs (PKWs) used a limited range of experimental data, which means, that they are inappropriate for wide parametric ranges, that might lead to significant errors. This study aimed to propose a reformed empirical equation using a wide range of data points gathered from previous experimental studies. Further, the appropriateness to use the existing equations for the collected data points, and the related errors, were investigated in detail using graphical and statistical analyses. The proposed equation predicted the discharge coefficients with < 5% absolute errors for 83.5% data points and with < 10% absolute errors for 100% data points, and the mean absolute error was 2.9%. Such variations may be attributed to the differences in experimental conditions that exist among the previous studies. The correlation indices were higher for the proposed equation as compared to the same for the existing equations, whereas the error indices were lowest for the proposed one. For some very specific parametric ranges, the existing equations still hold better accuracy. Overall, the proposed equation can precisely estimate the discharge coefficient of the basic geometry of Type-A PKWs for a wide parametric range and shall be handy in the hydraulic design of such PKWs.

Keywords: Piano key weir; Discharge coefficient; Empirical equation; Graphical analysis; Statistical analysis.

Introduction

One of the most crucial components of water resources projects is the hydraulic structures: dams, barrages, and weirs, which are built either to store or to divert the flow. These structures are safeguarded by passing the design flood through the spilling arrangements. Basically, the weirs are used for discharge control and measurement, channel stabilization, water level moderation, etc. According to Erpicum et al. (2021), the designs in hydraulic structures engineering are evolving continuously with innovations and new strategies to handle the problems related to human evolution. The consequences of global warming and cloud burst events are imposing upward revision of design flood discharge requirements and rehabilitation of many existing dams and diversion structures may be required for future sustainability. Traditionally, linear weirs, especially the ogee-crested weirs have been build and the application of non-linear weirs was limited till around 1970 (Crookston et al. 2019; Erpicum et al. 2021). In the first half of twentieth century, the labyrinth weir was proposed to counter the site or the project limitations and to increase the crest length (Crookston et al. 2019). Steady growth in the construction of labyrinth weirs have been observed over the past five decades. At the beginning of twenty-first century, another innovative solution – Piano key weir (PKW) was introduced by Lempérière and Ouamane (2003) to further enhance the specific discharge

q. PKWs have capability to pass higher specific discharges under lower water heads as compared to the other weirs. These novel type of modified labyrinth weirs have been used in the recent two decades in many dam rehabilitation projects, especially in France and Vietnam (Ho Ta Khanh 2017; Laugier et al. 2017). Although PKWs have been built mainly with low to medium sized dams, they have also been used with larger diversion discharge applications like Van Phong in Vietnam and Sawra Kuddu in India (Ho Ta Khanh 2017; Kumar et al. 2021a; b; Noseda et al. 2019). Crookston et al. (2019) identified thirty-four PKW constructions completed through 2019. Over the past two decades, the foremost research topic on PKWs has been the discharge capacity and the influence of related parameters as elaborated later. The current study proposes an analytical solution for the discharge coefficient C_{PK} of Type-A PKWs, which can be used precisely for a wide range of parameters than the existing equations.

Basic configuration

The basic parameters of PKWs are presented in Fig. 1, where P = weir height, W_i = inlet key width, W_o = outlet key width, B_i = inlet key overhang, B_o = outlet key overhang, B_b = base or footprint length, B = sidewall crest length, T_s = sidewall thickness, T_i = inlet crest thickness, T_o = outlet crest thickness, B_h = sidewall crest length measured between the outlet and the inlet crest axes, W = total width of the channel or the weir, P_d = dam height below the weir keys. In case of Type-A PKWs, $B_i = B_o$. In addition, the width of a PKW unit (or cycle) $W_u = W_i + W_o + 2T_s$ and the developed crest length of a PKW unit $L_u = W_u + 2B_h$. If N_u is the number of PKW units, then $W = N_u \times W_u$ and the total developed crest length $L = N_u \times L_u$. A naming convention for different parameters of PKW was suggested by Pralong et al. (2011) and it has been widely used. However, review of literature reveals that a total of three different crest planforms where used previously which affect the axes' locations and the design of the parameter B_h as shown in Figs. 1(a–c). Therefore, correct estimation of B_h is crucial to evaluate the discharge coefficient precisely as B_h directly affects L and eventually the L/W ratio. Furthermore, rounded values of some parameters (especially *L*, *W*, and *L/W*) are reported sometimes in the literature which can lead to some errors while formulating and evaluating the discharge coefficient equations.

Studies on the discharge capacity of Piano Key Weirs

The previous studies on the discharge capacity of PKWs were focused on (i) the basic geometry of PKWs, (ii) the influence of several parameters: weir height, crest length magnification ratio, key widths ratio, dam height, wall thickness, key overhangs ratio, submergence, and similar, and (iii) the effect of the crest shape and the addition of parapet walls and noses into the basic configuration. Anderson (2011); Anderson and Tullis (2013) studied the effect of W_i/W_o by varying it from 0.67 to 1.5 and found that PKW with W_i/W_o = 1.5 and 1.25 had higher C_{PK} than the other models and mentioned that a further increase in W_i/W_o can eventually decrease C_{PK}, especially for high heads. This finding is consistent with the observations of Machiels (2012); Machiels et al. (2014); Li et al. (2019) ; Shen and Oertel (2021). Machiels (2012); Machiels et al. (2014) observed an increase in the specific discharge with an increase in the weir height up to P/W_u = 1.3. A gain in C_{PK} with an increase in *L/W* was reported in several studies like Kabiri-Samani and Javaheri (2012); Leite Ribeiro et al. (2011); Noui and Ouamane (2011); Kumar et al. (2021a). The effect of *L/W* is significant at low to medium heads, but not so substantial at high heads when the effective crest length of PKW reduces due to the local submergence. The *H/P*, where *H* = total head over the weir crest (head above the weir crest *h* + velocity head), has been the most studied parameter and it can influence the effect of other geometric parameters: *L/W*, W_i/W_o, P/W_u etc., especially at high heads for which the local submergence has a greater influence. In addition, the effect of some modifications to the basic geometry have been studied previously. A parapet wall above the weir keys increases the weir height, helps to reduce the local submergence and the inlet loss (Anderson and Tullis 2013), and can enhance the discharge capacity of a basic PKW geometry as found by Anderson (2011); Anderson and Tullis (2013);

Karimi Chahartaghi et al. (2019); Machiels et al. (2013). However, such addition can only be effective up to a certain optimal height of the weir (Machiels et al. 2013). Furthermore, placement of noses below the upstream apexes can provide a smooth transition for the incoming flow and can reduce the inlet energy loss, and thus can improve the weir discharge capacity as reported by Anderson and Tullis (2013). Although Leite Ribeiro et al. (2007) observed no noticeable increase in the maximum discharge capacity (at the design head) by altering the crest shape, Anderson and Tullis (2013) detected noticeable enhancement in the discharge coefficient for a model with W_i/W_o = 1.25, especially at lower heads, when the flat top crest was replaced by the half-round crest. Unlike the flat top crest, the nappe clung to the upstream apex crest for the entire tested H in case of the half-round crest. However, the effectiveness of such nappe condition was gradually reduced with an increase in H which alters the local submergence in the outlet key. In addition, narrowing the sidewalls widen the keys and eventually increases the discharge capacity. Laugier et al. (2011) performed Computational Fluid Dynamics (CFD) simulations on PKW configurations with constant W_u while varying T_s from 0.02 m to 0.5 m and found a reduction in the discharge capacity with thickening of the sidewalls. However, the loss was generally reduced for higher heads as discussed by Laugier et al. (2011). PKWs have been built using concrete considering cost, maintenance, hydrodynamic vibration, and other related issues (Denys and Basson 2020; Laugier et al. 2011), except the Oule dam in France in which stainless steel was used (Crookston et al. 2019; Erpicum et al. 2017).

Existing equations and their limitations

As used by Kabiri-Samani and Javaheri (2012); Kumar et al. (2019, 2021a), the discharge capacity of a free-flowing PKW can be represented as:

$$Q = \frac{2}{3} C_{PK} W \sqrt{2gH^3} \tag{1}$$

where Q = discharge and g = acceleration due to gravity. Anderson and Tullis (2012a; b, 2013); Crookston et al. (2018) expressed the discharge capacity using the commonly used weir head-discharge relationship (Henderson 1966) which can be obtained by replacing $C_{PK}W$ with $C_d L$ in Eq. (1), where C_d = dimensionless discharge coefficient. Both the approaches are useful. However, in the present study, all data points were transformed in terms of W using Eq. (1). Kumar et al. (2019) previously evaluated the performance of the existing four equations suggested by Cicero and Delisle (2013); Crookston et al. (2018); Kabiri-Samani and Javaheri (2012) and Leite Ribeiro et al. (2012b), respectively and found that the equations proposed by Cicero and Delisle (2013) and Crookston et al. (2018) predicted the discharge coefficient with higher accuracies than the other two for a tested data range. Therefore, the appropriateness to use the equations suggested by Cicero and Delisle (2013) and Crookston et al. (2018) were only evaluated in the present study. Cicero and Delisle (2013) proposed the following equation for Type-A PKWs based on a polynominal fitting (written in terms of Eq. (1))

$$C_{PK} = \frac{3}{2}\left[1.63 + 0.59\left(\frac{H}{P}\right) - 11.56\left(\frac{H}{P}\right)^2 + 21.72\left(\frac{H}{P}\right)^3 - 12.46\left(\frac{H}{P}\right)^4\right] \tag{2}$$

Equation (2) is applicable for $0.1 < H/P < 0.72$. Later, Crookston et al. (2018) proposed the following equation for the discharge coefficient of nine PKW configurations based upon the data from Anderson (2011); Anderson and Tullis (2013) (written in terms of Eq. (1))

$$C_{PK} = \frac{L}{W}\left[1 \Big/ \left\{a + b\left(\frac{H}{P}\right) + c \Big/ \left(\frac{H}{P}\right)\right\} + d\right] \tag{3}$$

Where a, b, c, and d are coefficients which vary depending on the PKW configuration. For the basic configuration of Type-A PKWs, the corresponding coefficient values and the applicability of Eq. (3) are provided in Table 1. Equation (2) was formulated using a particular set of data points and lacks in accounting for the influence of L/W which is one of the most important parameters for PKWs, especially for low to medium H/P. It is also unable to reflect the effects of W_i/W_o and P/W_u. Therefore, this equation cannot precisely predict C_{PK} for a wide range of parameters. In view of this, the suitability of Eq. (2) was analyzed for $0.1 < H/P < 0.72$ and $4.3 \leq L/W \leq 5.08$ only. Whereas Eq. (3), proposed by Crookston et al. (2018), was formulated using experimental results collected for very specific values of L/W, P/W_u, and W_i/W_o and it lacks in considering the influences of L/W and P/W_u. The values of such parameters depend on the actual project site and can vary from one to another. For example, P/W_u = 1.3 and 0.5 were suggested for new and rehabilitation projects (Erpicum et al. 2017; Machiels 2012; Machiels et al. 2014). Similarly, based on the experience from 11 projects undertaken in France, Laugier et al. (2017) suggested L/W from 4 to 6 for new projects and even higher value of L/W (up to 7) for rehabilitation works. Furthermore, the prototype data obtained from thirty-four PKW prototypes (Crookston et al. 2019) indicate the requirement of analytical solutions which can be applied for wide parametric ranges.

The present study reformulates an empirical equation for the discharge coefficient of Type-A PKWs using data points which cover wide ranges of the main governing parameters H/P, L/W, P/W_u, and W_i/W_o. Thorough survey on the available data was carried out and eventually a total of 395 data points were collected from previous experimental studies. The proposed equation overcomes the limitations of the existing equations, does not limit its applicability for specific parametric values, and can be used efficiently in the planning and hydraulic design of the basic Type-A PKW geometry. However, the influence of parapet walls, noses below the upstream apexes, sidewall thickness, and crest shape are beyond the scope of this study.

Non-dimensional parameters

The discharge passing over a PKW under free-flow condition depends on flow, fluid, and weir geometry parameters. In case of a free-flowing PKW, the discharge capacity can be represented as:

$$Q = f\left(L_u, W_u, W_i, W_o, P, B_i, B_o, H, P_d, g, \rho, \sigma, \mu\right) \quad (4)$$

where *f* is a functional symbol, ρ = density of fluid, σ = surface tension of fluid, and μ = dynamic viscosity of fluid. Equation (4) can be represented in a non-dimensional form as:

$$C_{PK} = \varphi\left(\frac{L}{W}, \frac{H}{P}, \frac{W_i}{W_o}, \frac{P}{W_u}, \frac{B_i}{B_o}, \frac{P_d}{P}, \mathrm{We}, \mathrm{Re}\right) \quad (5)$$

where φ denotes another functional symbol, basically $L_u/W_u = L/W$, We is the Weber number = $\rho V^2 L_1/\sigma$, Re is the Reynolds number = $\rho V L_1/\mu$, V = characteristics velocity or reference velocity, and L_1 = characteristic length or reference length which can be considered as a function of H (Erpicum et al. 2016; Tullis et al. 2020). All data points, except the ones from Kabiri-Samani and Javaheri (2012) with B_o/B_i = 1.6, have equal overhangs, i.e. B_o/B_i = 1. Additionally, P_d/P values for the collected data points are either nil or small. Therefore, B_o/B_i and P_d/P were omitted from the analysis. Generally, a minimum H of 0.03 m is considered to be the criteria to eliminate the size scale effects related to viscous and surface tension forces (Erpicum et al. 2016; Kabiri-Samani and Javaheri 2012; Pfister et al. 2013). However, a recent comprehensive study carried out by Tullis et al. (2020) on a total of five PKW models of different prototype-to-model length ratios showed that there is no fixed value of either H or H/P above which the size-scale effects are negligible. In fact, the limiting value of H is lower for a smaller model than that for a bigger model, but H/P is higher for the smaller model than that for the bigger one. Considering the recommendations of Tullis et al. (2020), a minimum H/P of 0.15 (consistent with Shen and Oertel (2021)) and a minimum H of 0.02 m were found to be the suitable criteria for negligible size scale effects for the used data points. Furthermore, the studies dealt with turbulent flow and the viscous effect is small as compared to the gravity. Therefore, We and Re were also removed from the analysis. Finally, Eq. (5) simplifies to

$$C_{PK} = \phi\left(\frac{L}{W}, \frac{H}{P}, \frac{W_i}{W_o}, \frac{P}{W_u}\right) \quad (6)$$

Elucidation of the Collected Data

A total of 395 data points were congregated from previous studies. The basic geometric parameters and the ranges of non-dimensional parameters are provided in Tables 2 and 3, respectively. Anderson (2011); Anderson and Tullis (2013) conducted a series of experiments on nine PKW configurations in a 7.32 m long, 0.933 m wide, and 0.61 m deep flume using calibrated orifice meters (accuracy of ± 0.2%) and a stilling well assembly (with readability ≈ 0.15 mm). Out of those nine configurations, three (with W_i/W_o = 1.0, 1.25, and 1.5) were used in the present study. Cicero and Delisle (2013) studied the discharge capacities of different PKW types under both free and submerged flow conditions in a 25 m long flume using an electromagnetic flow meter (accuracy of ± 1%) and the piezometric head measurements (accuracy of ± 0.18 mm). The data points from the case of free-flowing Type-A PKW were used here. Denys and Basson (2020) conducted experiments in a 1.5 m wide and 20 m long flume using electromagnetic flow meter (accuracy of ± 0.5%), point gauge (precision of 0.1 mm), and pitot tube (precision of 1 mm). Kabiri-Samani and Javaheri (2012) carried out experiments on thirty PKW configurations in a 12 m long, 0.4 m wide, and 0.7 m deep flume using a point gauge (precision of 0.1 mm) and the discharge measured with precision of 0.1 l/s. The results of two relevant configurations were used in this investigation. Kumar et al. (2019) conducted experiments in a 15 m long, 0.39 m wide, and 0.5 m deep tilting flume using ultrasonic flowmeter (accuracy of ± 1%) and point gauge (least count of 0.1 mm). Leite Ribeiro et al. (2011) investigated the influence of dam height (P_d/P) on the variation in discharge enhancement ratio against H/P in a 2 m wide channel having a 0.5 m wide PKW section within it. They reported a few results for the case with no dam height (P_d/P = 0) which were used in the present study. Li et al. (2020) studied the flow characteristics of PKW by performing CFD simulations in Ansys-Fluent and by conducting experiments in a 16 m long, 0.5 m wide, and 0.75 m deep flume using electromagnetic flow meter (accuracy of ± 1%), water level gauge (accuracy of ± 0.1 mm), and Vernier gauge (accuracy of ± 0.5 mm). Machiels (2012); Machiels et al. (2011, 2014) conducted studies in a 7.2 m long, 1.2 m wide, and 1.2 m deep flume using electromagnetic flow meter (accuracy of ± 1×10^{-3} m^3/s) and gauge or ultrasonic probe (accuracy of ± 0.5 mm). In these studies, the PKW sections were either 0.6 m or 0.75 m wide. Noui and Ouamane (2011) conducted experiments on PKWs by placing the models at a location that had an upstream basin of 1.1 m deep and 3m × 3m plan section and a downstream channel of 1 m width. Tullis et al. (2020) carried out experiments on five PKW models in different flumes using magnetic or orifice plate flow meters (accuracy of ± 0.25%), point gauges (accuracy of ± 0.15 mm), and stilling wells. Shen and Oertel (2021) conducted a series of experiments on twenty PKW configurations in a 10 m long, 0.3 m wide, and 0.5 m deep glass walled flume using calibrated magnetic flowmeters (accuracy of ± 0.3%) and point gauge (accuracy of ± 0.1 mm). The datapoints from two of the tested configurations with W_i/W_o = 1.5 were used in the present analysis. There are more studies available on Type-A PKWs in Leite Ribeiro et al. (2012a; b); Machiels et al. (2014). However, either the head-discharge data or some of the required parameters are not present in those cases, and therefore, no useful data points could be collected. Moreover, the collected datapoints belong to the range: L/W ~ 4 to 6 with average = 4.948, H/P ~ 0.15 to 1.6 (and H > 0.02 m) with average = 0.503, W_i/W_o ~ 1 to 1.57 with average = 1.312, and P/W_u ~ 0.5 to 1.333 with average = 0.868. These parametric values are mostly comparable to the prototype data (especially from the new projects) obtained by Crookston et al. (2019) from thirty-four PKW prototypes. In addition, all the collected data points, except the ones from Leite Ribeiro et al. (2011) (with semi-circular crest), were apparently recorded for flat top crest PKW models. Besides, 353 data points out of the total 395 were within a narrow range of W_u/T_s, from 15.3 to 21.67. Therefore, the effect of T_s seems insignificant for the tested data. The remaining 42 data points were collected from Kabiri-

Samani and Javaheri (2012) with W_u/T_s = 200, Noui and Ouamane (2011) with W_u/T_s = 196.1, and Li et al. (2020) with W_u/T_s = 50.

Results and discussion

Reformed equation

The collected 395 data points were utilized and the following equation was formulated using the non-linear regression approach

$$C_{PK} = 0.327\left(\frac{L}{W}\right)^{0.669}\left(\frac{H}{P}\right)^{-0.487}\left(\frac{W_i}{W_o}\right)^{0.276}\left(\frac{P}{W_u}\right)^{-0.171} \quad \left(\mathrm{R}^2 = 0.979\right) \tag{7}$$

Equation (7) is applicable for a wide range of data points: L/W ~ 4 to 6, H/P ~ 0.15 to 1.6 (and H > 0.02 m), W_i/W_o ~ 1 to 1.57, and P/W_u ~ 0.5 to 1.333.

Graphical analysis for the proposed and the available equations

Out of the total 395 data points, 256 data points (for $0.15 < H/P < 0.72$ and $4.3 \le L/W \le 5.08$) were used to check the appropriateness of Eq. (2) and 368 data points (for $0.15 \le H/P \le 0.9$ or 1.0 depending on the value of W_i/W_o) were used in case of Eq. (3), respectively. For W_i/W_o values up to 1.5, the coefficients in Eq. (3) were obtained by linear interpolation using the coefficients provided for W_i/W_o = 1.0, 1.25, and 1.5 in Table 1. Whereas for W_i/W_o = 1.57, the coefficients were approximated to be the same as those for W_i/W_o = 1.5. Figures 2(a-b) and Fig. 3 show variations in the calculated C_{PK} against the observed C_{PK} for the existing equations, Eqs. (2) and (3), and for the proposed Eq. (7), respectively. It was found that Eq. (3) could predict C_{PK} with relatively smaller errors (mean absolute percentage error, MAPE = 2.64%) for the data points with L/W around 5.0 (also see Table 3), excluding the data points from Machiels et al. (2014) for which the MAPE was 8.64%. This observation is attributed to the effect of parameter P/W_u which is absent in Crookston et al. (2018). Besides, Fig. 2(a) shows that for most of the data points with L/W values other than ~ 5 (also see Table 3), Eq. (3) could still estimate the higher C_{PK} values, i.e., at lower H/P, with lower errors (within ± 10%) than the lower C_{PK} values at higher heads (errors within about ± 15%). However, an opposite scenario was observed for the data points from Machiels et al. (2011) with P/W_u = 1.313 which again indicates the effect of P/W_u. Furthermore, C_{PK} was overestimated for higher L/W values and was underestimated for lower L/W values, except the data points from Machiels et al. (2011) with L/W = 4.03. The observations reflect that the rate of reduction in the effective crest length with an increase in H/P due to the local submergence is dissimilar for different L/W, and thus, C_{PK} could not be estimated accurately while considering a linear variation with L/W, especially for higher heads. Therefore, the equation proposed by Crookston et al. (2018) is appropriate for L/W around 5.0 when P/W_u is around 0.9, and may also be suitable for other L/W values when H/P is lower. Figure 2(b) shows that Eq. (2) could still predict C_{PK} with lower errors (within ± 10%) for most of the data points (74.2% as discussed later) in the range $4.3 \leq L/W \leq 5.08$, even though the equation was proposed based on L/W = 4.61. However, C_{PK} was underestimated for higher C_{PK} values, i.e., at lower heads, at which the influence of L/W dominates that of H/P. Furthermore, for the data points from Machiels et al. (2014), higher errors (MAPE = 9.27% and maximum error = 15.58%) were observed which is primarily due to the influence of P/W_u. In contrast, Fig. 3 shows that the proposed Eq. (7) predicted C_{PK} with comparatively lower errors than the available equations (from Fig. 2) and most of the data points (83.5% as discussed later) were within ± 5% error range. Such improvements were achieved by the presence of P/W_u together with the other basic non-dimensional parameters. Still, at lower H/P, especially for $0.15 < H/P < 0.16$, some of the predictions had an error close to 10% which can be partly caused by the higher measurement uncertainties at lower heads and partly due to the inability of the proposed power function to represent the change in the curvature of C_{PK} at H/P around that range which was observed previously (Anderson and Tullis 2013; Crookston et al. 2018; Tullis et al. 2020). At such lower H/P values, the equation proposed by Crookston et al. (2018), Eq. (3), can be a suitable choice. In addition, for the data points from Leite Ribeiro et al. (2011) with semi-circular crest, it was found that the existing equations and the proposed equation predicted C_{PK} with lower absolute errors, < 3.7% only. All other data points apparently belong to flat top crest PKW models. Therefore, the semi-circular crest had insignificant effect on the present study.

A closer comparison between the predicted C_{PK} and the observed C_{PK} for the data points from Cicero and Delisle (2013); Anderson and Tullis (2013), which were used to formulate the existing equations, Eqs. (2) and (3), respectively, is shown in Fig. 4. Both the existing, Eq. (3), and the proposed, Eq. (7), equations predicted C_{PK} with marginal errors (within about ± 6%) for the data points from Anderson and Tullis (2013). Furthermore, the MAPE values for Eq. (7) and Eq. (3) were 2.4% and < 1%, respectively. However, for the data points from Cicero and Delisle (2013), Eq. (7) estimated C_{PK} with comparatively higher errors (mostly from 8% to 9%), and the MAPE values for Eq. (7) and Eq. (2) were 7.1% and < 1%, respectively. For the same data points, Eq. (3) also estimated C_{PK} with a similar error pattern (mostly from 8% to 10%) than that of Eq. (7) as can be seen in Fig. 2(a). Since the proposed Eq. (7) was expressed based on a wide parametric range taken from several studies with different experimental conditions and different measurement uncertainties, the observed MAPE values are likely.

The used 256 data points for Eq. (2), 368 data points for Eq. (3), and 395 data points for Eq. (7) were sorted separately by ascending orders of the absolute percent errors. Then the percentile score of the number of data points were plotted (see Fig. 5) against the sorted absolute percentage errors for further graphical inspection on the performance of these equations in addition to what was observed from Figs. 2 – 3. It was found that the proposed Eq. (7) estimated 83.5% data points with < 5% absolute error, whereas the same was 48.4% and 50.5% for Eqs. (2) and (3), respectively. Similarly, C_{PK} values for 100%, 74.2%, and 76.1%

data points were predicted within ± 10% error range by Eqs. (7), (2), and (3), respectively. Furthermore, the maximum error values were found to be 9.97%, 15.58%, and 16.37% for these three equations, respectively. These observations also indicate that Eq. (7) is preferred over Eqs. (2) and (3) for a wide parametric range.

Statistical analysis for the proposed and the available equations

The accuracy of the proposed equation and the usability of the existing equations for the tested parametric ranges (as discussed in the graphical analysis) were further analyzed using several statistical parameters: mean absolute error (MAE), MAPE, mean square error (MSE), root mean square error (RMSE), percentage sum of the squares of the error (SSE%), coefficient of correlation (CC), and efficiency of correlation (E^2) (Ahmad 2013; Kadia et al. 2020; Kumar et al. 2019; Maier and Dandy 1996; Pandey et al. 2015; Rajurkar et al. 2004; Sheppard et al. 2014). Equations (8) – (14) show the expressions of these statistical parameters, where Y = observed C_{PK}, $\overline{Y}$ = mean of the observed C_{PK}, and Y' = calculated C_{PK} (Ahmad 2013; Pandey et al. 2015; Rajurkar et al. 2004; Sheppard et al. 2014). The calculated values are provided in Table 4. It was found that the correlation indices (CC and E^2) are higher and the error indices (MAE, MAPE, MSE, RMSE, and SSE%) are lower for the proposed Eq. (7) as compared to the other two. For example, the RMSE and the MAPE values for the proposed Eq. (7) were 0.062 and 2.9%, respectively which are comparatively lower than the same for Eq. (2) – 0.137 and 6.12%, respectively, and for Eq. (3) – 0.118 and 5.89%, respectively. The MAPE of 2.9% seems reasonable considering the difference in the experimental conditions among the previous studies.

$$\mathrm{MAE} = \frac{1}{n}\sum_{i=1}^{n}\left|Y_i - Y_i'\right| \tag{8}$$

$$\mathrm{MAPE} = \frac{100}{n}\sum_{i=1}^{n}\frac{\left|Y_i - Y_i'\right|}{\left|Y_i\right|} \tag{9}$$

$$\mathrm{MSE} = \frac{1}{n}\sum_{i=1}^{n}\left(Y_i - Y_i'\right)^2 \tag{10}$$

$$\mathrm{RMSE} = \sqrt{\frac{\sum_{i=1}^{n}\left(Y_i - Y_i'\right)^2}{n}} \tag{11}$$

$$\mathrm{SSE\%} = 100\frac{\sum_{i=1}^{n}\left(Y_i - Y_i'\right)^2}{\sum_{i=1}^{n}\left(Y_i\right)^2} \tag{12}$$

$$\mathrm{CC} = \frac{n\sum_{i=1}^{n}Y_iY_i' - \sum_{i=1}^{n}Y_i\sum_{i=1}^{n}Y_i'}{\sqrt{n\sum_{i=1}^{n}Y_i^2 - \left(\sum_{i=1}^{n}Y_i\right)^2}\sqrt{n\sum_{i=1}^{n}Y_i'^2 - \left(\sum_{i=1}^{n}Y_i'\right)^2}} \tag{13}$$

$$\mathrm{E}^2 = \frac{\sum_{i=1}^{n}\left(Y_i - \overline{Y}\right)^2 - \sum_{i=1}^{n}\left(Y_i - Y_i'\right)^2}{\sum_{i=1}^{n}\left(Y_i - \overline{Y}\right)^2} \tag{14}$$

Performance of the equations for different ranges of the non-dimensional parameters

For the tested overall parametric ranges, both the graphical and the statistical analyses showed precise estimation of C_{PK} using the proposed Eq. (7) and presented the appropriateness of the other two equations. However, the analysis was not limited only to the overall data points but also extended to different ranges of the non-dimensional parameters: L/W, H/P, W_i/W_o, and P/W_u to check the usability of equations for different parametric ranges. Firstly, for L/W, the used data points: 256 for Eq. (2), 368 for Eq. (3) and 395 for Eq. (7) were split separately into three ranges: $L/W < 4.9$, $4.9 \leq L/W < 5.1$, and $L/W \geq 5.1$, respectively. Figure 6(a) shows that the proposed Eq. (7) performed reasonably well for all L/W ranges as the corresponding MAPE values were from 2.7% to 4.4% only. Still, Eq. (2) appears to be suitable for $4.3 \leq L/W < 4.9$, provided that the data has a P/W_u value close to that of Cicero and Delisle (2013) (see Table 3). Application of Eq. (2) to the data from Machiels et al. (2011) with $L/W = 4.03$ and $P/W_u =$

1.313 would lead to an overestimation of C_{PK} by about 25% to 30%, primarily due to P/W_u followed by L/W. Furthermore, it was found that Eq. (3) is suitable for $4.9 \leq L/W < 5.1$ when P/W_u is around 0.9. Similarly, the data points were split into five ranges of H/P as indicated in Fig. 6(b). It was found that Eq. (7) predicted C_{PK} with marginal MAPE (around 3% only) for the used ranges. Whereas the tested data points for the existing equations showed MAPE values from 4.4% to 8.8% for Eq. (3) and 4.9% to 6.6% for Eq. (2), respectively, which are higher primarily due to the absence of P/W_u in those equations. Furthermore, at lower H/P, especially for $0.15 < H/P < 0.16$, some data scatter was observed for Eq. (7), and the equation proposed by Crookston et al. (2018), Eq. (3), is a suitable choice for such range of H/P. In addition, Figs. 6(c–d) show the prediction accuracies for different ranges of W_i/W_o and P/W_u. It was found that the proposed Eq. (7) predicted C_{PK} with lowest MAPE for all ranges of W_i/W_o and P/W_u. For $W_i/W_o \sim 1.25$, all three equations predicted C_{PK} with lower errors (MAPE ≤ 5%) than the other W_i/W_o ranges. It happened primarily because the variation in P/W_u was lower for the data points with $W_i/W_o \sim 1.25$ than the other two ranges as can be observed from Table 3. Therefore, the inclusion of P/W_u in Eq. (7) improved the prediction precisions. Furthermore, Fig. 6(d) shows that Eq. (3) could still predict C_{PK} with marginal errors (MAPE = 4.1%) for $0.7 \leq P/W_u < 0.9$. A further inspection revealed that Eq. (3), proposed by Crookston et al. (2018), is appropriate for P/W_u around 0.9, especially if L/W is around 5.0 – also discussed in the graphical analysis.

Sensitivity analysis for the non-dimensional parameters

The sensitivity analysis for the proposed Eq. (7) was performed for the four input parameters: L/W, H/P, W_i/W_o, and P/W_u using the collected 395 data points to recognize the most influential parameter. The sensitivity and the error analyses were executed using the average values of the input parameters, using the corresponding value of C_{PK}, and considering the errors in each input parameter to be independent as suggested by Ahmad (2013). For the collected data points, the computed average values of the input parameters (X): L/W, H/P, W_i/W_o, and P/W_u were 4.948, 0.503, 1.312, and 0.868, respectively and the corresponding C_{PK} was 1.471. During the sensitivity analysis, each of those four average input values were varied individually by ± 10% (marked as ΔX) and the corresponding changes in the discharge coefficient (ΔC_{PK}) were determined as provided in Table 5.

For all eight cases, the sensitivity was determined using three indices: absolute sensitivity AS = $\Delta C_{PK}/\Delta X$, relative error RE = $\Delta C_{PK}/C_{PK}$, and relative sensitivity RS = $(X \times \Delta C_{PK})/(C_{PK} \times \Delta X)$ as used by Ahmad (2013). Table 5 shows the values obtained from different cases. The obtained ΔC_{PK}, RE, and RS values indicate that L/W is the most important and sensitive input parameter amongst the four, followed by H/P, W_i/W_o, and P/W_u, respectively. The relative sensitivity of L/W was about 1.29 to 1.45 times that of H/P, 2.37 to 2.47 times that of W_i/W_o, and 3.74 to 4.07 times that of P/W_u, respectively. However, the absolute sensitivity was highest for H/P, which indicates that only a slight absolute variation in H/P can cause a large deviation in C_{PK}, and therefore, precise measurement of the head over the weir crest is crucial.

Conclusions

Previously, researchers proposed equations for the estimation of C_{PK} based on limited experimental data. Those equations are suitable for specific parametric ranges and would lead to significant errors if applied to wide parametric ranges, as observed. Furthermore, previously used three different crest planforms can affect the L/W ratio. Sometimes, rounded values of certain parameters (especially L/W) are reported in the literature. Therefore, careful observations on the selection of crest configuration and L/W value are crucial in a comparison study and in studies which deal with equations and data from other studies. This study aimed to formulate a precise empirical equation for the discharge coefficient of Type-A PKWs using available data which cover a wide range of parameters to overcome the limitations of the existing equations. A total of 395 data points were gathered, and Eq. (7) was formulated.

Besides, the possibility to apply the existing equations to the parametric ranges beyond their own data was analyzed in detail. Both graphical and statistical analyses (using 256 data points for Eq. (2), 368 for Eq. (3), and 395 for Eq. (7)) were performed to check the precision in C_{PK} predictions. Equation (7) predicted 83.5% and 100% data points with < 5% and < 10% absolute error values, respectively. The statistical analysis showed that the correlation indices were highest for Eq. (7) and the error indices were lowest. For example, the RMSE and MAPE values for Eq. (7) were 0.062 and 2.9% only, but the same values for Eq. (2) were 0.137 and 6.12% and for Eq. (3) were 0.118 and 5.89%, respectively. Mainly, the inclusion of P/W_u in the reformed Eq. (7) improved the predictions significantly. The MAPE of 2.9% is reasonable considering the differences in the experimental conditions present among the previous studies. Furthermore, L/W was found to be the most sensitive input parameter for C_{PK} followed by H/P, W_i/W_o, and P/W_u, respectively. The relative sensitivity of L/W was about 1.29 to 1.45 times that of H/P and was even higher for the other two parameters W_i/W_o and P/W_u. Additionally, for different parametric ranges of the data, the proposed equation estimated C_{PK} with marginal errors (maximum MAPE was 4.4%). Yet, Eq. (2) proposed by Cicero and Delisle (2013) was found appropriate for $4.3 \leq L/W < 4.9$, when $P/W_u \sim 0.7$; and the equation suggested by Crookston et al. (2018), Eq. (3), was found appropriate for $L/W \sim 5.0$ and $H/P < 1.0$, when $P/W_u \sim 0.9$. Moreover, the proposed Eq. (7) is suitable for a wide range of parameters: $L/W \sim$ 4 to 6, $H/P \sim$ 0.15 to 1.6, $W_i/W_o \sim$ 1 to 1.57, and $P/W_u \sim$ 0.5 to 1.333 which are comparable to the prototype data provided in Crookston et al. (2019), especially to the data from new projects. Therefore, the reformed equation shall be advantageous in planning and hydraulic design of the basic geometry of Type-A PKWs placed at diversion works and at low dams. However, the effects of parapet walls, noses beneath the upstream apexes, crest shape, wall thickness, and dam height (for high P_d/P) were not in the scope of the proposed equation; and it is further recommended to use the proposed equation for flat top crest configurations and for sidewall thickness in the range of $15.3 \leq W_u/T_s \leq 21.67$. Meanwhile, these effects can be evaluated numerically for the basic geometry and the possibility of further improvements on the proposed equation can be explored.

Data Availability Statement

The data points collected from Kumar et al. (2019) are available from the corresponding author upon reasonable request. All other data points were obtained from the published manuscripts.

Acknowledgement

This study is supported by NTNU (project number 81772024). The authors would like to thank all researchers whose data helped greatly in this study.

Conflicts of interests

The authors have no conflicts of interests.

Notations

B = Sidewall crest length (m);

B_b = Base or footprint length (m);

B_i = Inlet key overhang (m);

B_o = Outlet key overhang (m);

B_h = Sidewall crest length measured between the outlet and the inlet crest axes (m);

C_d = Dimensionless discharge coefficient (-);

C_{PK} = Discharge coefficient of PKW in terms of channel width (-);

H = Total upstream head over the weir crest including the velocity head (m);

L = Total developed crest length of the weir (m);

L_u = Total developed crest length of a PKW unit or cycle (m);

N_u = Number of PKW units or cycles (-);

P = Weir height (m);

P_d = Dam height below the weir keys (m);

Q = Discharge (m^3/s);

q = Specific discharge (m^2/s);

T_i = Inlet crest thickness (m);

T_o = Outlet crest thickness (m);

T_s = Sidewall thickness (m);

W = Total width of the channel or the weir (m);

W_i = Inlet key width (m);

W_o = Outlet key width (m);

W_u = Width of a PKW unit or cycle (m);

References

Ahmad, Z. (2013). "Prediction of longitudinal dispersion coefficient using laboratory and field data: relationship comparisons." *Hydrology Research*, 44(2), 362–376.

Anderson, R. M. (2011). "Piano key weir head discharge relationships." Mater of Science Thesis, Civil and Environmental Engineering, Utah State University, Logan, Utah.

Anderson, R. M., and Tullis, B. P. (2012a). "Comparison of Piano Key and Rectangular Labyrinth Weir Hydraulics." *Journal of Hydraulic Engineering*, 138(4), 358–361.

Anderson, R. M., and Tullis, B. P. (2012b). "Piano Key Weir: Reservoir versus Channel Application." *Journal of Irrigation and Drainage Engineering*, 138(8), 773–776.

Anderson, R. M., and Tullis, B. P. (2013). "Piano Key Weir Hydraulics and Labyrinth Weir Comparison." *Journal of Irrigation and Drainage Engineering*, 139(3), 246–253.

Cicero, G. M., and Delisle, J. R. (2013). “Discharge characteristics of piano key weirs under submerged flow.” *Proceedings of the Second International Workshop on Labyrinth and Piano Key Weirs -PKW 2013, Paris, France,* CRC Press, London, 101–109.

Crookston, B. M., Anderson, R. M., and Tullis, B. P. (2018). “Free-flow discharge estimation method for Piano Key weir geometries.” *Journal of Hydro-environment Research*, 19, 160–167.

Crookston, B. M., Erpicum, S., Tullis, B. P., and Laugier, F. (2019). “Hydraulics of Labyrinth and Piano Key Weirs: 100 Years of Prototype Structures, Advancements, and Future Research Needs.” *Journal of Hydraulic Engineering*, 145(12), 02519004.

Denys, F. J. M. (2019). “Investigation into Flow-induced Vibrations of Piano Key Weirs.” Doctor of Philosophy Dissertation, Stellenbosch University.

Denys, F. J. M., and Basson, G. R. (2020). “Unsteady Hydrodynamic Behavior at Piano Key Weirs.” *Journal of Hydraulic Engineering*, 146(5), 04020028.

Erpicum, S., Archambeau, P., Dewals, B., and Pirotton, M. (2017). “Hydraulics of Piano Key Weirs: A review.” *Proceedings of the 3rd International Workshop on Labyrinth and Piano Key Weirs (PKW 2017), Qui Nhon, Vietnam*, CRC Press, London, 27–36.

Erpicum, S., Crookston, B. M., Bombardelli, F., Bung, D. B., Felder, S., Mulligan, S., Oertel, M., and Palermo, M. (2021). “Hydraulic structures engineering: An evolving science in a changing world.” *Wiley Interdisciplinary Reviews: Water*, 8(2), e1505.

Erpicum, S., Tullis, B. P., Lodomez, M., Archambeau, P., Dewals, B. J., and Pirotton, M. (2016). “Scale effects in physical piano key weirs models.” *Journal of Hydraulic Research*, 54(6), 692–698.

Henderson, F. M. (1966). *Open channel flow*. Macmillan, New York.

Ho Ta Khanh, M. (2017). “History and development of Piano KeyWeirs in Vietnam from 2004 to 2016.” *Proceedings of the 3rd International Workshop on Labyrinth and Piano Key Weirs (PKW 2017), Qui Nhon, Vietnam*, CRC Press, London, 3–16.

Kabiri-Samani, A., and Javaheri, A. (2012). “Discharge coefficients for free and submerged flow over Piano Key weirs.” *Journal of Hydraulic Research*, 50(1), 114–120.

Kadia, S., Kumar, B., and Ahmad, Z. (2020). “Discharge Characteristics of Triangular Weir with Upstream Ramp and Its CFD Modelling Using Ansys CFX Module.” *Recent Trends in Environmental Hydraulics. GeoPlanet: Earth and Planetary Sciences*, M. B. Kalinowska, M. M. Mrokowska, and P. M. Rowiński, eds., Springer, Cham, 77–90.

Karimi Chahartaghi, M., Nazari, S., and Shooshtari, M. M. (2019). “Investigating the effect of a parapet wall on the hydraulic performance of an arced piano key weir.” *Journal of Hydraulic Research*, 58(2), 274–282.

Kumar, B., Kadia, S., and Ahmad, Z. (2019). “Evaluation of discharge equations of the piano key weirs.” *Flow Measurement and Instrumentation*, 68, 101577.

Kumar, B., Kadia, S., and Ahmad, Z. (2021a). “Discharge Characteristics of Piano Key Weirs With and Without Upstream Siltation.” *International Journal of Civil Engineering*, 19(9), 1043–1054.

Kumar, B., Kadia, S., and Ahmad, Z. (2021b). “Sediment Movement over Type-A Piano Key Weirs.” *Journal of Irrigation and Drainage Engineering*, 147(6), 04021018.

Laugier, F., Pralong, J., and Blancher, B. (2011). “Influence of structural thickness of sidewalls on PKW spillway discharge capacity.” *Proc. of the International Conference on Labyrinth and Piano Key Weirs - PKW2011, Liege, Belgium*, CRC Press, London, 159–165.

Laugier, F., Vermeulen, J., and Blancher, B. (2017). “Overview of design and construction of

11 Piano Key Weirs spillways developed in France by EDF from 2003 to 2016.” *Proceedings of the 3rd International Workshop on Labyrinth and Piano Key Weirs (PKW 2017), Qui Nhon, Vietnam*, CRC Press, London, 37–51.

Leite Ribeiro, M., Bieri, M., Boillat, J. L., Schleiss, A. J., Singhal, G., and Sharma, N. (2012a). “Discharge Capacity of Piano Key Weirs.” *Journal of Hydraulic Engineering*, 138(2), 199–203.

Leite Ribeiro, M., Boillat, J.-L., Schleiss, A. J., Le Doucen, O., and Laugier, F. (2011). “Experimental parametric study for hydraulic design of PKWs.” *Proceedings of the International Conference on Labyrinth and Piano Key Weirs -PKW 2011*, CRC Press, London, 183–190.

Leite Ribeiro, M., Boillat, J.-L., Schleiss, A. J., Laugier, F., and Albalat, C. (2007). “Rehabilitation of St-Marc Dam Experimental Optimization of a Piano Key Weir.” *Proceedings of the 32nd Congress of IAHR*, International Association for Hydraulic Research, Madrid, Spain.

Leite Ribeiro, M., Pfister, M., Schleiss, A. J., and Boillat, J. L. (2012b). “Hydraulic design of a-type piano key weirs.” *Journal of Hydraulic Research*, 50(4), 400–408.

Lempérière, F., and Ouamane, A. (2003). “The Piano Keys weir: A new cost-effective solution for spillways.” *International Journal on Hydropower and Dams*, 10(5), 144–149.

Li, G., Li, S., and Hu, Y. (2019). “The effect of the inlet/outlet width ratio on the discharge of piano key weirs.” *Journal of Hydraulic Research*, 58(4), 594–604.

Li, S., Li, G., and Jiang, D. (2020). “Physical and Numerical Modeling of the Hydraulic Characteristics of Type-A Piano Key Weirs.” *Journal of Hydraulic Engineering*, 146(5), 06020004.

Machiels, O. (2012). “Experimental study of the hydraulic behaviour of Piano Key Weirs.” PHD thesis, HECE, Faculty of Applied Science, University of Liège, Liège.

Machiels, O., Erpicum, S., Archambeau, P., Dewals, B., and Pirotton, M. (2013). “Parapet Wall Effect on Piano Key Weir Efficiency.” *Journal of Irrigation and Drainage Engineering*, 139(6), 506–511.

Machiels, O., Erpicum, S., Dewals, B. J., Archambeau, P., and Pirotton, M. (2011). “Experimental observation of flow characteristics over a Piano Key Weir.” *Journal of Hydraulic Research*, 49(3), 359–366.

Machiels, O., Pirotton, M., Pierre, A., Dewals, B., and Erpicum, S. (2014). “Experimental parametric study and design of Piano Key Weirs Experimental parametric study and design of Piano Key Weirs.” *Journal of Hydraulic Research*, 52(3), 326–335.

Maier, H. R., and Dandy, G. C. (1996). “The Use of Artificial Neural Networks for the Prediction of Water Quality Parameters.” *Water Resources Research*, 32(4), 1013–1022.

Noseda, M., Stojnic, I., Pfister, M., and Schleiss, A. J. (2019). “Upstream Erosion and Sediment Passage at Piano Key Weirs.” *Journal of Hydraulic Engineering*, 145(8), 04019029.

Noui, A., and Ouamane, A. (2011). “Study of optimization of the Piano Key Weir.” *Proceedings of the International Conference on Labyrinth and Piano Key Weirs -PKW 2011*, CRC Press, London, 175–182.

Pandey, M., Ahmad, Z., and Sharma, P. K. (2015). “Estimation of maximum scour depth near a spur dike.” *Canadian Journal of Civil Engineering*, 43(3), 270–278.

Pfister, M., Battisacco, E., Cesare, G. De, and Schleiss, A. J. (2013). “Scale effects related to the rating curve of cylindrically crested Piano Key weirs.” *Proceedings of the Second International Workshop on Labyrinth and Piano Key Weirs -PKW 2013, Paris, France,* CRC Press, London, 73–82.

Pralong, J., Vermeulen, J., Blancher, B., Laugier, F., Erpicum, S., Machiels, O., Pirotton, M., Boillat, J.-L., Leite Ribeiro, M., and Schleiss, A. J. (2011). “A naming convention for the Piano KeyWeirs geometrical parameters.” *Proceedings of the International Conference on Labyrinth and Piano Key Weirs - PKW2011, Liege, Belgium*, CRC Press, London, 271–278.

Rajurkar, M. P., Kothyari, U. C., and Chaube, U. C. (2004). “Modeling of the daily rainfall-runoff relationship with artificial neural network.” *Journal of Hydrology*, 285(1–4), 96–113.

Shen, X., and Oertel, M. (2021). “Comparative Study of Nonsymmetrical Trapezoidal and Rectangular Piano Key Weirs with Varying Key Width Ratios.” *Journal of Hydraulic Engineering*, 147(11), 04021045.

Sheppard, D. M., Melville, B., and Demir, H. (2014). “Evaluation of Existing Equations for Local Scour at Bridge Piers.” *Journal of Hydraulic Engineering*, 140(1), 14–23.

Tullis, B. P., Crookston, B. M., and Young, N. (2020). “Scale Effects in Free-Flow Nonlinear Weir Head-Discharge Relationships.” *Journal of Hydraulic Engineering*, 146(2), 04019056.

Young, N. L. (2018). “Size-scale effects of nonlinear weir hydraulics.” Mater of Science Thesis, Civil and Environmental Engineering, Utah State University, Logan, Utah.

586 **Tables**

587 **Table 1.** Coefficients and applicability of Eq. (3) proposed by Crookston et al. (2018) [with permission from Elsevier]

For W_i/W_o	a	b	c	d	Applicability
1.0	0.5091	10.29	0.09712	0.1164	$0.1 \leq H/P \leq 0.9$
1.25	0.4216	9.412	0.1027	0.1114	$0.1 \leq H/P \leq 0.9$
1.5	0.4895	8.4	0.09448	0.09608	$0.1 \leq H/P \leq 1.0$

Table 2. Summary of basic geometric parameters and specific discharge for the collected data points

Investigators	$^c q$ (× 10^{-2} m^2/s)	P (m)	W_i (m)	W_o (m)	T_s (m)	$T_i = T_o$ (m)	$B_o = B_i$ (m)	B (m)	B_h (m)	W_u (m)	L_u (m)	N_u (-)
(Anderson 2011; Anderson and Tullis 2012a, 2013)	3.9 – 25.5	0.1969	0.1247, 0.1156, 0.1039	0.0833, 0.0925 0.1039	0.0127		0.1214	0.489	0.4763	0.2334, 0.2335, 0.2332	1.186	4
Cicero and Delisle (2013)	5.1 – 23.4	0.222	0.133	0.133	0.02		0.154	0.573	0.553	0.306	1.412	6.5
Denys (2019); Denys and Basson (2020)	12.4 – 41.5	0.4	0.3	0.24	0.03		0.27	1.02	0.99	0.6	2.58	2.5
Kabiri-Samani and Javaheri (2012)	7.5 – 21.3	0.25	0.099, 0.109	0.099, 0.089	[a]0.001		*	0.5	0.499	0.2	1.198	2
Kumar et al. (2019)	1.9 – 6.8	0.105	0.059	0.059	0.006	0	0.064	0.254	0.254	0.13	0.638	3
Leite Ribeiro et al. (2011)	8.6 – 30.4	0.217	0.163	0.13	[a]0.02		0.23	0.67	0.65	0.333	1.633	1.5
Li et al. (2020)	3 – 22	0.125	0.1333	0.1067	0.005	0	0.125	0.5	0.5	0.25	1.25	2
Machiels et al. (2011); Machiels (2012)	12.7 – 49.2	0.525	0.18	0.18	0.02	0.024	0.184	0.63	0.606	0.4	1.612	1.5
Machiels (2012); Machiels et al. (2014)	4 – 41.5	0.4, 0.3, 0.24, 0.2, 0.15	0.165	0.105	0.015	0	0.2	0.6	0.6	0.3	1.5	2.5
Noui and Ouamane (2011)	3.9 – 16.2	0.15	0.09	0.075	[a, b]0.00085		0.103	0.41	0.40915	0.1667	0.985	6
Shen and Oertel (2021)	2.3 – 10	0.1, 0.2	0.054, 0.108	0.036, 0.072	0.005, 0.01		na	0.2, 0.4	0.195, 0.39	0.1, 0.2	0.49, 0.98	3, 1.5
Tullis et al. (2020); Young (2018)	1.8 – 126.1	0.8372, 0.4186, 0.2791, 0.1395, 0.0698	0.4968, 0.2484, 0.1656, 0.0828, 0.0414	0.3866, 0.1933, 0.1289, 0.0644, 0.0322	0.0539, 0.027, 0.018, 0.009, 0.0045		0.5156, 0.2578, 0.1719, 0.086, 0.043	2.0766, 1.0383, 0.6922, 0.3461, 0.1731	2.0226, 1.0113, 0.6742, 0.3371, 0.1686	0.9913, 0.4957, 0.3305, 0.1652, 0.0826	5.0366, 2.5183, 1.6789, 0.8394, 0.4197	2

a: considering $T_i = T_o = T_s$, b: calculated from the reported W_i, W_o, and W_u values, c: calculated in most cases, na: not available, *: B_o = 0.08 m and B_i = 0.05 m

Table 3. Range of non-dimensional parameters for the collected data points

Investigators	L/W	H/P	W_i/W_o	P/W_u
Anderson and Tullis (2013)	5.08	0.152 – 0.927	1.0, 1.25, 1.5	0.844
Cicero and Delisle (2013)	4.61	0.175 – 0.719	1.0	0.725
Denys and Basson (2020)	4.3	0.174 – 0.548	1.25	0.667
Kabiri-Samani and Javaheri (2012)	5.99	0.169 – 0.526	1.0, 1.225	1.25
Kumar et al. (2019)	4.9	0.197 – 0.704	1.0	0.808
Leite Ribeiro et al. (2011)	4.9	0.271 – 0.973	1.254	0.652
Li et al. (2020)	5.0	0.21 – 1.558	1.25	0.5
Machiels et al. (2011)	4.03	0.16 – 0.541	1.0	1.313
Machiels et al. (2014)	5.0	0.152 – 1.602	1.571	0.5 – 1.333
Noui and Ouamane (2011)	5.91	0.195 – 0.878	1.2	0.9
Shen and Oertel (2021)	4.9	0.15 – 1.021	1.5	1.0
Tullis et al. (2020)	5.08	0.152 – 0.999	1.285	0.845

Table 4. Performance of equations

Equation	MAE	MAPE (%)	MSE	RMSE	SSE (%)	CC	E^2
Eq. (2) (Cicero and Delisle 2013)	0.11	6.12	0.0186	0.137	0.576	0.942	0.856
Eq. (3) (Crookston et al. 2018)	0.095	5.89	0.0139	0.118	0.473	0.96	0.91
Eq. (7) (Proposed)	0.047	2.9	0.0039	0.062	0.139	0.988	0.977

Table 5. Sensitivity and error analysis for different input parameters affecting the proposed equation, Eq. (7)

X	ΔX	For 10% increment in X				For 10% reduction in X			
		ΔC_{PK}	AS	RE	RS	ΔC_{PK}	AS	RE	RS
L/W	0.4948	0.0968	0.196	0.0658	0.658	-0.1001	-0.202	-0.0681	-0.681
H/P	0.0503	-0.0667	-1.326	-0.0454	-0.454	0.0774	1.539	0.0526	0.526
W_i/W_o	0.1312	0.0392	0.299	0.0267	0.267	-0.0422	-0.321	-0.0287	-0.287
P/W_u	0.0868	-0.0238	-0.274	-0.0162	-0.162	0.0267	0.308	0.0182	0.182

Figures

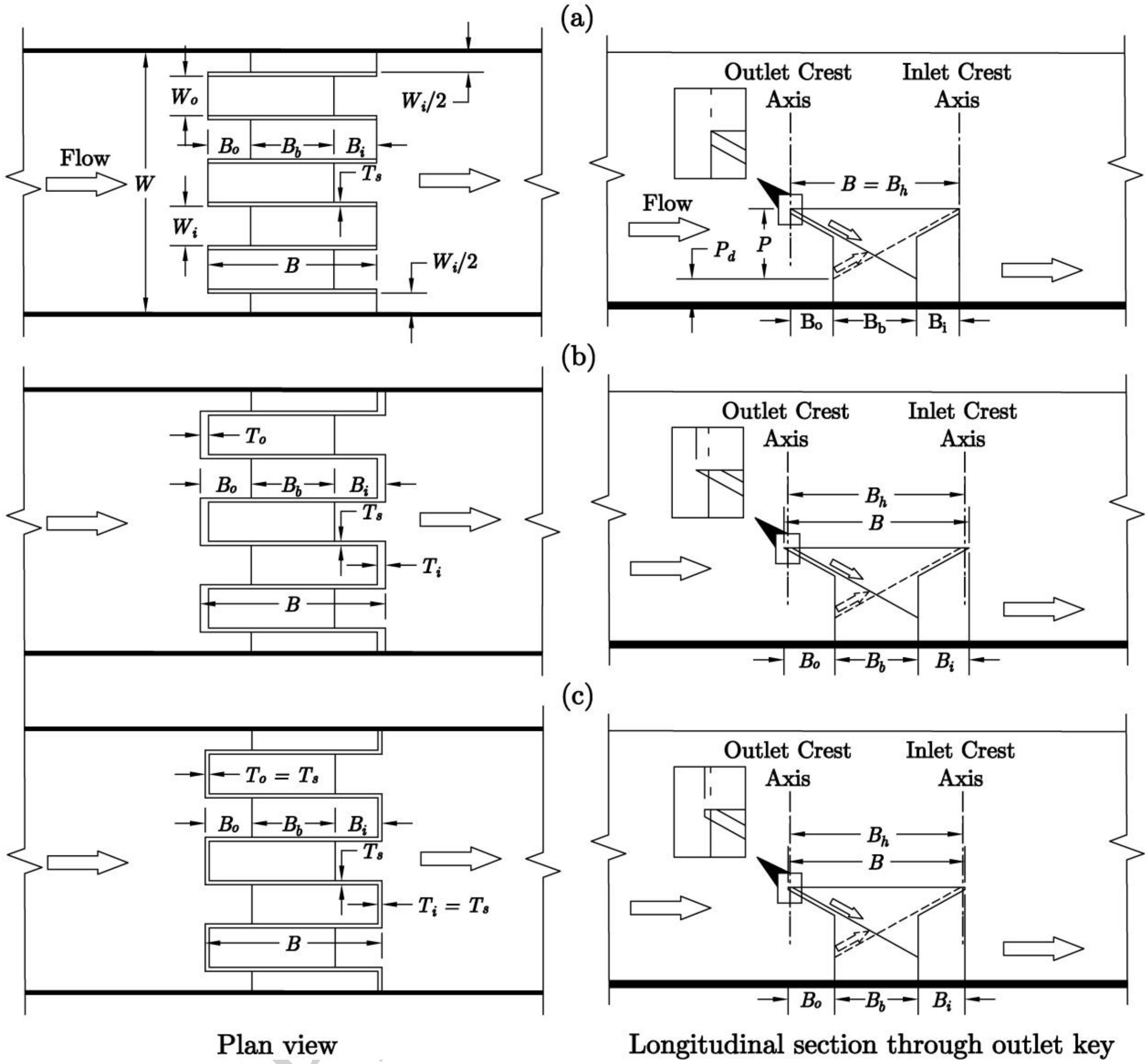

Fig. 1. Different components of a PKW with: (a) $B_h = B$ (Kumar et al. 2019, 2021a; b; Li et al. 2020; Machiels et al. 2011; Machiels 2012); (b) $B_h = B - 0.5\ (T_i + T_o)$ (Machiels et al. 2011; Machiels 2012); (c) $B_h = B - T_s$ (Anderson and Tullis 2012a, 2013; Denys and Basson 2020; Shen and Oertel 2021; Tullis et al. 2020)

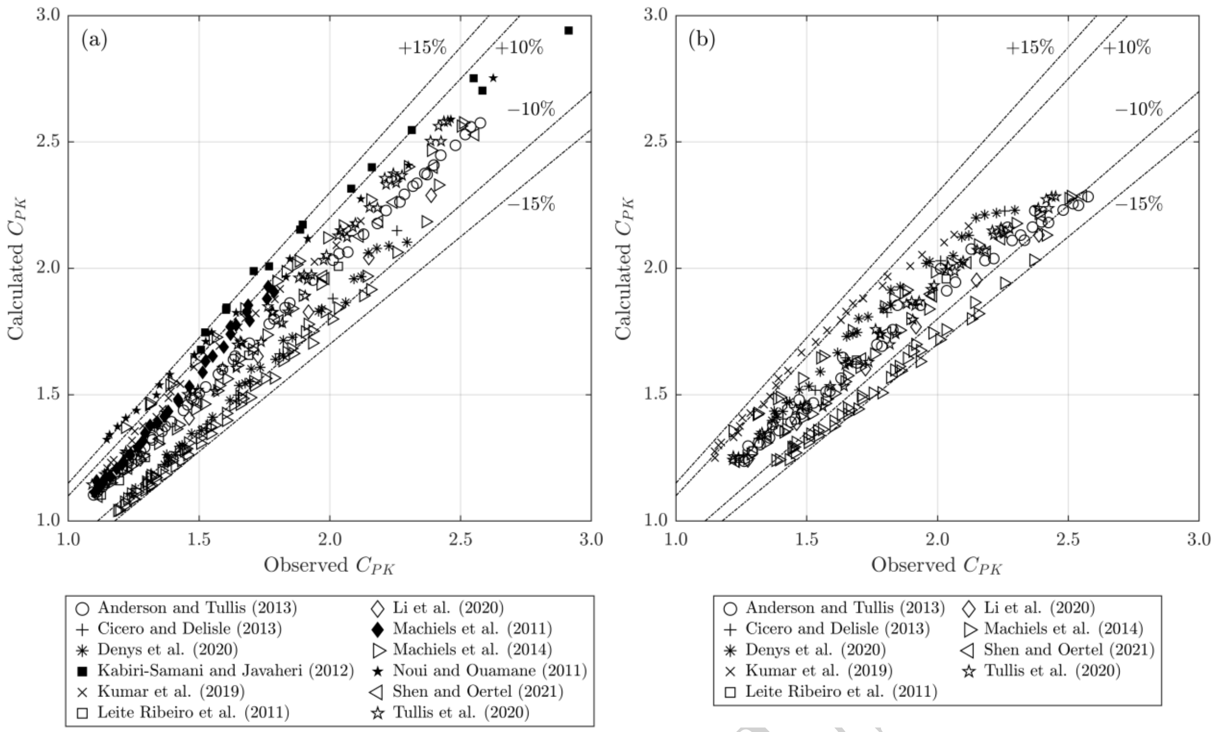

Fig. 2. Calculated C_{PK} versus Observed C_{PK} for the existing equations: (a) Eq. (3); (b) Eq. (2)

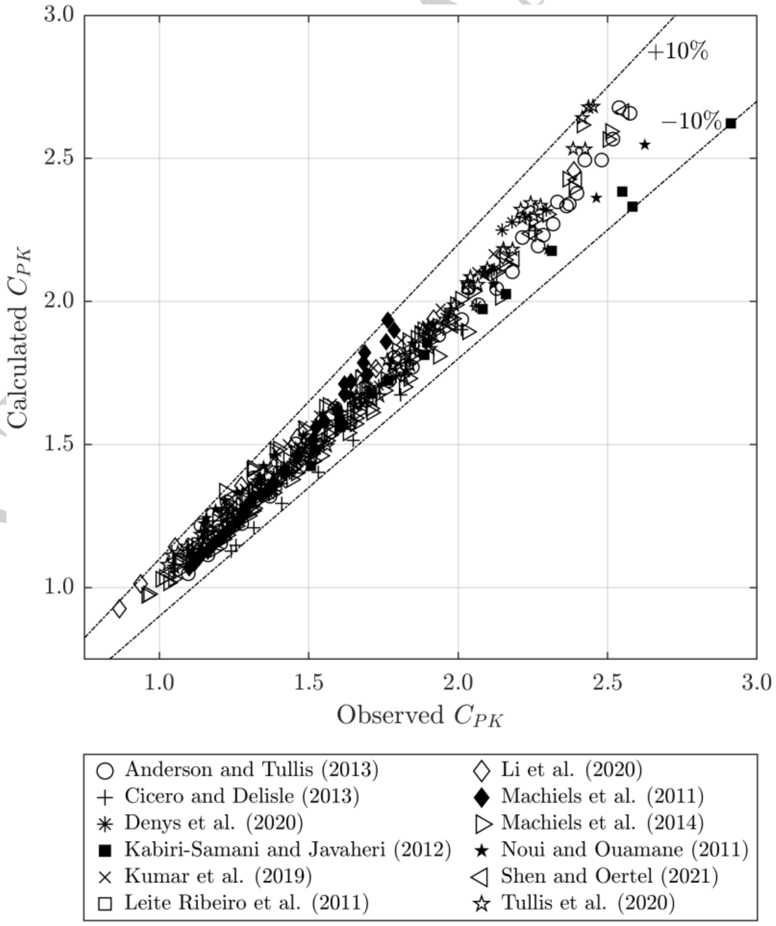

Fig. 3. Calculated C_{PK} versus Observed C_{PK} for the proposed Eq. (7)

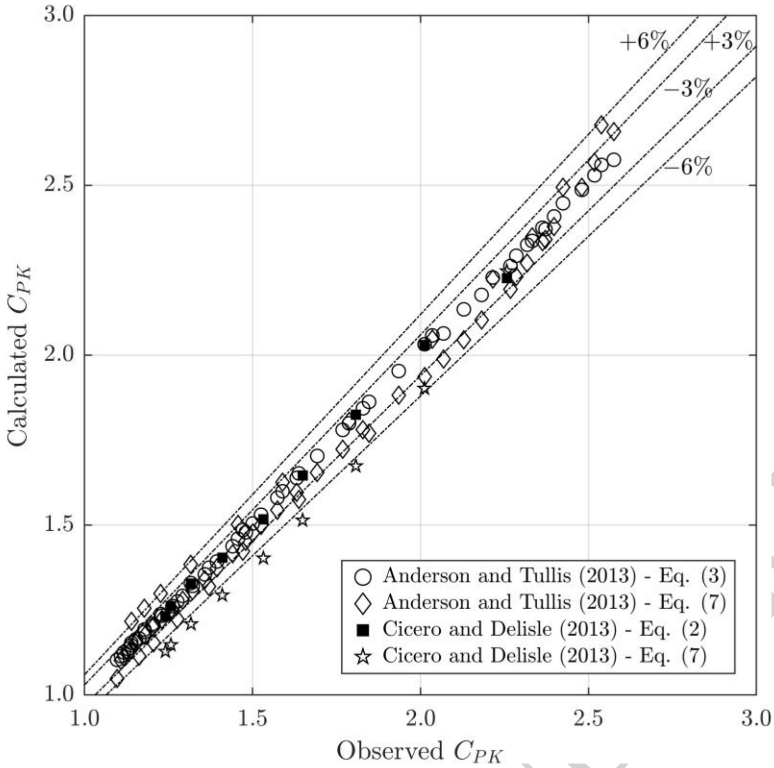

Fig. 4. Calculated C_{PK} versus Observed C_{PK} for the data points used to formulate the existing equations, Eq. (2) and (3) (see also Table 3)

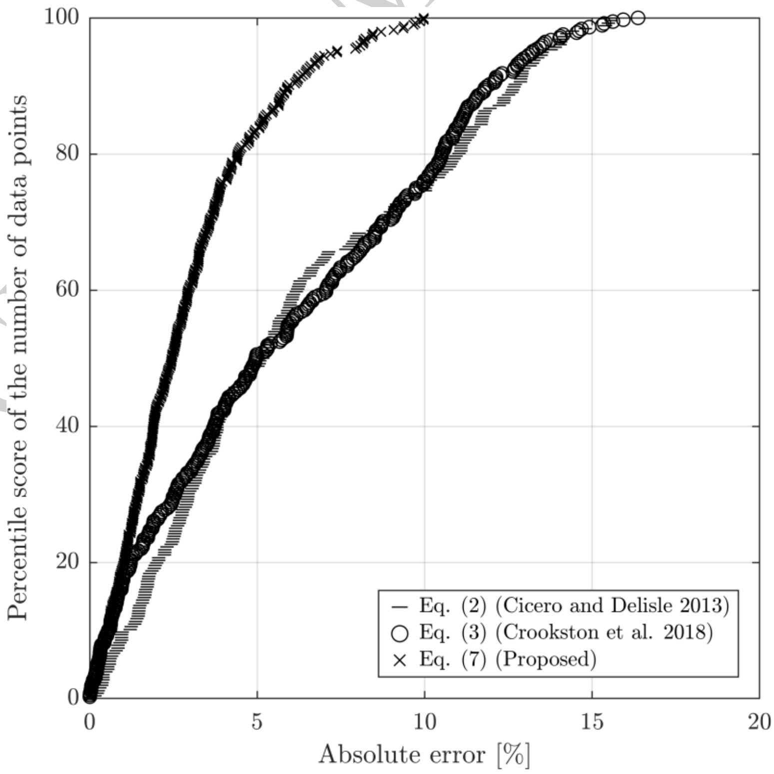

Fig. 5. Variation in the percentile score of the number of data points against the absolute percentage error for the proposed and the exiting equations

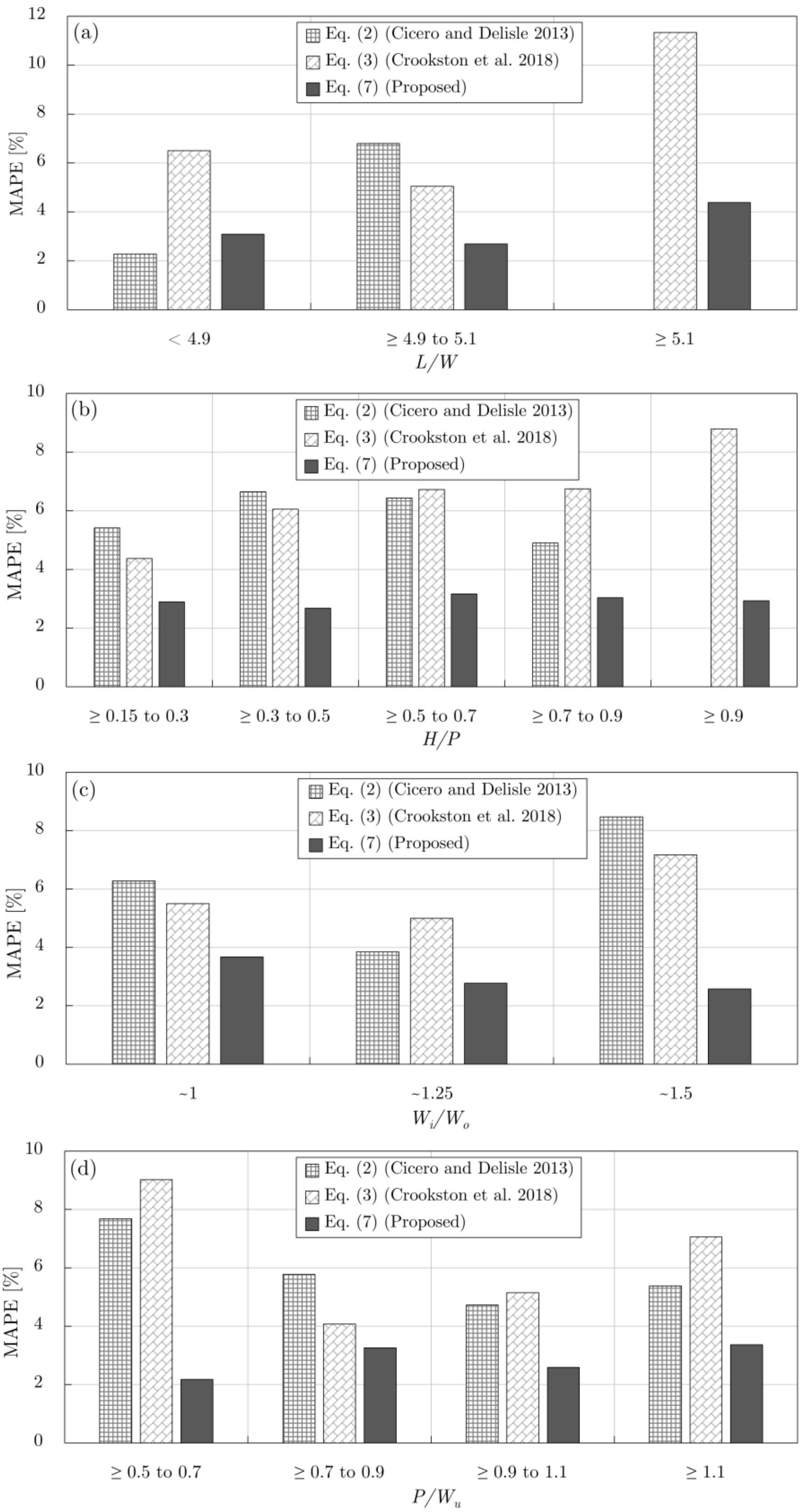

Fig. 6. Efficiency of proposed and existing equations for different ranges of: (a) *L/W*; (b) *H/P*; (c) W_i/W_o; (d) P/W_u